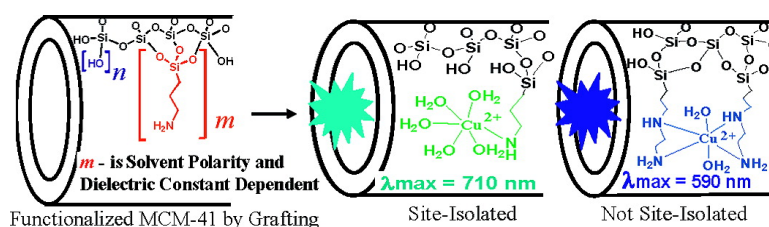


Toward Efficient Nanoporous Catalysts: Controlling Site-Isolation and Concentration of Grafted Catalytic Sites on Nanoporous Materials with Solvents and Colorimetric Elucidation of Their Site-Isolation

Krishna K. Sharma, Abhishek Anan, Robert P. Buckley, Wayne Ouellette, and Tewodros Asefa

J. Am. Chem. Soc., **2008**, 130 (1), 218-228 • DOI: 10.1021/ja074128t • Publication Date (Web): 13 December 2007

Downloaded from <http://pubs.acs.org> on March 19, 2009



More About This Article

Additional resources and features associated with this article are available within the HTML version:

- Supporting Information
- Links to the 2 articles that cite this article, as of the time of this article download
- Access to high resolution figures
- Links to articles and content related to this article
- Copyright permission to reproduce figures and/or text from this article

[View the Full Text HTML](#)

Toward Efficient Nanoporous Catalysts: Controlling Site-Isolation and Concentration of Grafted Catalytic Sites on Nanoporous Materials with Solvents and Colorimetric Elucidation of Their Site-Isolation

Krishna K. Sharma, Abhishek Anan, Robert P. Buckley, Wayne Ouellette, and Tewodros Asefa*

Department of Chemistry, Syracuse University, Syracuse, New York 13244

Received June 19, 2007; E-mail: tasefa@syr.edu

Abstract: We report that the polarity and dielectric constants of solvents used for grafting organosilanes on mesoporous materials strongly affect the concentration of grafted organic groups, the degree of their site-isolation, and the catalytic properties of the resulting materials. Polar and nonpolar organosilanes as well as polar-protic, dipolar-aprotic, and nonpolar solvents were investigated. Polar-protic solvents, which have high dielectric constants, resulted in smaller concentrations ($\sim 1\text{--}2$ mmol/g) of polar organic groups such as 3-aminopropyl groups, higher surface area materials, site-isolated organic groups, and more efficient catalytic properties toward the Henry reaction of *p*-hydroxybenzaldehyde with nitromethane. On the other hand, dipolar-aprotic and nonpolar solvents resulted in larger concentrations ($\sim 2\text{--}3$ mmol/g) of grafted polar functional groups, lower-to-higher surface area materials, more densely populated catalytic groups, and poor-to-efficient catalytic properties toward the Henry reaction. Both the polar-protic and dipolar-aprotic solvents resulted in significantly lower concentration of grafted groups for nonpolar organosilanes such as (3-mercaptopropyl)trimethoxysilane compared to corresponding grafting of the polar amino-organosilanes. The relationship between the solvent properties and the percentage and degree of site-isolation of the grafted functional groups was attributed to differences in solvation of the organosilanes and silanols in various solvents and possible hydrogen-bonding between the organosilanes and the solvents. The degree of site-isolation of the amine groups, which affect the material's catalytic properties, was elucidated by a new colorimetric method involving probing of the absorption maxima (λ_{max}) on the d-d electronic spectrum of Cu^{2+} complexes with the amine-functionalized materials and the colors of the samples. The absorption λ_{max} and the colors of the materials were found to be uniquely dependent on the type of solvents used for grafting the organoamines. For instance, the monoamine- and diamine-functionalized samples grafted in methanol resulted in pale blue and light purple colors with λ_{max} at ~ 720 and 650 nm, respectively. These correspond to CuNO_5 and CuN_2O_4 structures, respectively, which are indicative of the presence of site-isolated organoamines in samples grafted in methanol. The monoamine and diamine samples grafted in toluene resulted in purple and deep purple colors with λ_{max} at ~ 590 and 630 nm, respectively. These correspond to CuN_2O_4 and CuN_4O_2 , which are indicative of the presence of closely spaced organoamines in samples grafted in toluene. The samples grafted in isopropanol gave colors and λ_{max} intermediate between those of samples grafted in toluene and methanol.

1. Introduction

The functionalization of solid-state nanoporous materials with organic and organometallic moieties has proven to be an important step for the transformation of these materials into heterogeneous catalysts,^{1,2} sensors,³ efficient adsorbents,^{4,5} nanoelectronics and nanophotonics devices,⁶ and chromatographic supports.^{7,8} Since their discovery,^{9,10} mesoporous materials have been used as ideal host materials for various organic¹¹ and organometallic guest functional groups as well as metallic nanoparticles^{12,13} and nanowires¹⁴ due to their tunable, highly ordered nanometer pore structures and high surface areas and pore volumes. The three most commonly used methods for the synthesis of organic-functionalized mesoporous materials have

been (1) the co-assembly of terminal organosilanes with tetraalkoxysilanes,^{15,16} (2) the grafting of organosilanes onto the surfaces of mesoporous silica,¹⁷ and (3) the self-assembly of bridging organosilanes into periodic mesoporous organosilica

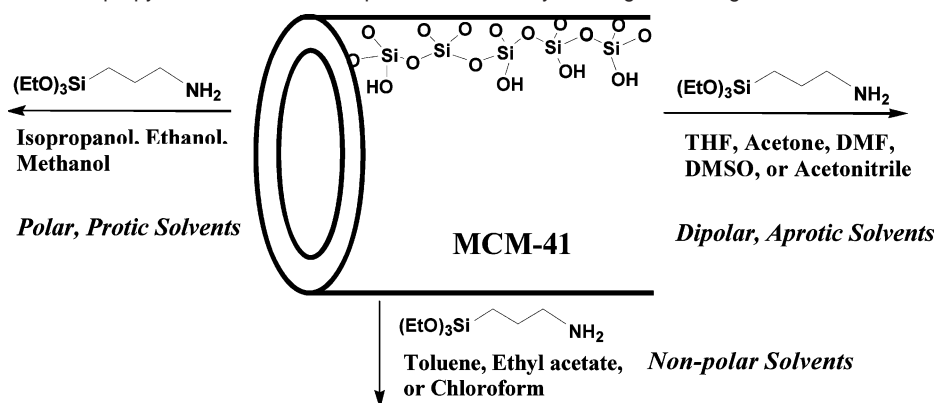
- (1) (a) Crudden, C. M.; Sateesh, M.; Lewis, R. *J. Am. Chem. Soc.* **2005**, *127*, 10045–10050. (b) Ying, J. Y.; Mehnert, C. P.; Wong, M. S. *Angew. Chem., Int. Ed.* **1999**, *38*, 56–77. (c) Brunel, D.; Blanc, A. C.; Galarneau, A.; Fajula, F. *Catal. Today* **2002**, *73*, 139–152. (d) Yang, H.; Gao, H.; Angelici, R. J. *Organometallics* **2000**, *19*, 622–629. (e) Balaji, T.; El-Safty, S. A.; Matsunaga, H.; Hanaoka, T.; Mizukami, F. *Angew. Chem., Int. Ed.* **2006**, *45*, 1–7. (f) Corma, A. *Chem. Rev.* **1997**, *97*, 2373–2420. (g) Heilmann, J.; Maier, W. F. *Angew. Chem., Int. Ed.* **1994**, *33*, 471–473. (h) Zapilk, C.; Liang, Y.; Nerdal, W.; Anwander, R. *Chem. Eur. J.* **2007**, *13*, 3169–3176. (i) Chiker, F.; Launay, F.; Nogier, J. P.; Bonardet, J. L. *Green Chem.* **2003**, *5*, 318–322. (j) Shimada, T.; Kurazono, R.; Morihara, K. *Bull. Chem. Soc. Jpn.* **1993**, *66*, 836–838. (k) Brunel, D. *Microporous Mesoporous Mater.* **1999**, *27*, 329–344. (l) Sayari, A. *Chem. Mater.* **1996**, *8*, 1840–1852.

(PMO) structures.^{18,19} In the grafting synthesis, organic functional groups are anchored by reacting various organosilanes with the silanol groups of parent mesoporous silica²⁰ and organosilica^{19f} materials. While in most reports the grafting of organosilanes was performed in nonpolar solvents, mainly toluene,²¹ we recently reported the synthesis of organic-functionalized mesoporous materials by grafting organosilanes

in a polar solvent, ethanol.²² Although our approach resulted in a lower number of immobilized organic groups compared to the corresponding grafting in toluene, it produced materials with better structures and properties including higher surface area, possibly more site-isolated organocatalytic sites, and unprecedented enhanced catalytic properties.²² It is also worth noting that our synthetic strategy left many residual silanol groups, which may be involved in acid–base cooperative catalysis of various reactions.²³ Silanols in organoamine-functionalized mesoporous materials were proposed to participate in various reactions catalyzed by these amino-functionalized mesoporous catalysts.^{24,25} Despite our successful strategy for synthesis of efficient catalysts by grafting amino-organosilanes on mesoporous silica in ethanol, to the best of our knowledge, the grafting of organosilanes in many other polar and nonpolar solvents with different polarity and dielectric constants and the correlations between the solvents' properties and the structures and catalytic properties of the resulting materials have not been systematically investigated so far.

On the other hand, although the site-isolation of organic groups and active catalytic sites on solid substrates is essential in many catalytic processes, the degree of site-isolation of grafted organic groups in many previously reported bifunctional catalysts²⁶ has also not been fully investigated.²⁷ For instance, it is known that enzymatic²⁸ and synthetic multifunctional²⁹ catalytic processes forming various biologically active chemicals and synthetic products, respectively, take place by the synergistic and cooperative participation of multiple, site-isolated functional

- (2) (a) Belser, T.; Stöhr, M.; Pfaltz, A. *J. Am. Chem. Soc.* **2005**, *127*, 8720–8731. (b) Copéret, C. *New J. Chem.* **2004**, *28*, 1–27. (c) Bartz, M.; Küther, J.; Seshadri, R.; Tremel, W. *Angew. Chem., Int. Ed.* **1998**, *110*, 2466–2468.
- (3) (a) Yuliarto, B.; Zhou, H.-S.; Yamada, T.; Honma, I.; Katsumura, Y.; Ichihara, M. *Anal. Chem.* **2004**, *76*, 6719–6726. (b) Balaji, T.; El-Safty, S. A.; Matsunaga, H.; Hanaoka, T.; Mizukami, F. *Angew. Chem., Int. Ed.* **2006**, *45*, 7202–7208. (c) Goettmann, F.; Moores, A.; Boissiere, C.; Le Floch, P.; Sanchez, C. *Small* **2005**, *1*, 636–639. (d) Basabe-Desmonts, L.; Reinhoudt, D. N.; Crego-Calama, M. *Chem. Soc. Rev.* **2007**, *36*, 993–1017. (e) Stevens, N.; Akins, D. L. *Sens. Actuators B* **2007**, *123*, 59–64. (f) Yamada, T.; Zhou, H.-S.; Uchida, H.; Tomita, M.; Ueno, Y.; Ichino, T.; Honma, I.; Asai, K.; Katsube, T. *Adv. Mater.* **2002**, *14*, 812–815. (g) Mortari, A.; Maarouf, A.; Martin, D.; Cortie, M. B. *Sens. Actuators B* **2007**, *123*, 262–268. (h) Tao, S.-Y.; Li, G.-T.; Zhu, H.-S. *J. Mater. Chem.* **2006**, *16*, 4521–4528. (i) Balaji, T.; Sasidharan, M.; Matsunaga, H. *Anal. Bioanal. Chem.* **2006**, *384*, 488–494.
- (4) (a) Lam, K.-F.; Yeung, K.-L.; McKay, G. *Langmuir* **2006**, *22*, 9632–9641. (b) Kargol, M.; Zajac, J.; Jones, D. J.; Roziere, J.; Steriotis, T.; Jimenez-Lopez, A.; Rodriguez-Castellon, E. *Chem. Mater.* **2005**, *17*, 6117–6127. (c) Yan, Z.; Li, G.-T.; Mu, L.; Tao, S.-Y. *J. Mater. Chem.* **2006**, *16*, 1717–1725.
- (5) Feng, X.; Fryxell, G.-E.; Wang, L.-Q.; Kim, A.-Y.; Liu, J.; Kemner, K.-M. *Science* **1997**, *276*, 923–926.
- (6) (a) Miyata, H.; Suzuki, T.; Fukuoka, A.; Sawada, T.; Watanabe, M.; Noma, T.; Takada, K.; Mukaike, T.; Kuroda, K. *Nat. Mater.* **2004**, *3*, 651–656. (b) Fukumoto, H.; Nagano, S.; Kawatsuki, N.; Seki, T. *Chem. Mater.* **2006**, *18*, 1226–1234. (c) Herance, J. R.; Peris, E.; Vidal, J.; Bourdelande, J. L.; Marquet, J.; Garcia, H. *Chem. Mater.* **2005**, *17*, 4097–4102. (d) Li, D.-L.; Zhou, H.-S.; Honma, I. *Nat. Mater.* **2004**, *3*, 65–72. (e) Antonelli, D. M.; Ying, J. Y. *Curr. Opin. Colloids Interface Sci.* **1996**, *1*, 523–529. (f) Wu, C.-G.; Bein, T. *Science* **1994**, *266*, 1013–1015. (g) Scott, B. J.; Wirmsberger, G.; Stucky, G. D. *Chem. Mater.* **2001**, *13*, 3140–3150. (h) Gross, A. F.; Diehl, M. R.; Beverly, K. C.; Richman, E. K.; Tolbert, S. H. *J. Phys. Chem. B* **2003**, *107*, 5475–5482. (i) Tsung, C.-K.; Hong, W.-B.; Shi, Q.-H.; Kou, X.-S.; Yeung, M.-H.; Wang, J.-F.; Stucky, G.-D. *Adv. Funct. Mater.* **2006**, *16*, 2225–2230. (j) Carreon, M. A.; Guliants, V. V. *Eur. J. Inorg. Chem.* **2005**, *27*–43. (k) Henning, T.; Brandner, J. J.; Eichhorn, L.; Schubert, K.; Schreiber, M.; Gungerich, M.; Gunther, H.; Klar, P. J.; Rebbin, V.; Fröba, M. *Microfluidics Nanofluidics* **2007**, *3*, 299–305.
- (7) (a) Gallis, K. W.; Araujo, J. T.; Duff, K. J.; Moore, J. G.; Landry, C. C. *Adv. Mater.* **1999**, *11*, 1452–1455. (b) Raimondo, M.; Perez, G.; Sinibaldi, N.; DeStefanis, A.; Tomlinson, A. A. *G. Chem. Commun.* **1997**, 1343–1344. (c) Minakuchi, H.; Nakanishi, K.; Soga, N.; Ishizuka, N.; Tanaka, N. *Anal. Chem.* **1996**, *68*, 3498–3501. (d) Grossmann, F.; Ehwald, V.; von Hohenesche, C. D.; Unger, K. K. *J. Chromatogr. A* **2001**, *910*, 223–236. (e) Katiyar, A.; Pinto, N. G. *Small* **2006**, *2*, 644–648. (f) Gritti, F.; Guiochon, G. *J. Chromatogr. A* **2005**, *1070*, 1–12.
- (8) (a) Han, Y.; Lee, S. S.; Ying, J. Y. *Chem. Mater.* **2007**, *19*, 2292–2298. (b) Lin, V. S.-Y.; Lai, C.-Y.; Huang, J.-G.; Song, S.-A.; Xu, S. *J. Am. Chem. Soc.* **2001**, *123*, 11510–11511. (c) Murata, S.; Furukawa, H.; Kuroda, K. *Chem. Mater.* **2001**, *13*, 2722–2729.
- (9) Kresge, C. T.; Leonowicz, M. E.; Roth, W. J.; Vartuli, J. C.; Beck, J. S. *Nature* **1992**, *359*, 710–712.
- (10) Yang, P.; Zhao, D.; Margolese, D. I.; Chmelka, B. F.; Stucky, G. D. *Nature* **1998**, *396*, 152–155.
- (11) (a) Tian, Z.-R.; Tong, W.; Wang, J.-Y.; Duan, N.-G.; Krishnan, V. V.; Suib, S. L. *Science* **1997**, *276*, 926–930. (b) Sayari, A.; Hamoudi, S. *Chem. Mater.* **2001**, *13*, 3151–3168. (c) Stein, A.; Melde, B. J.; Schroden, R. C. *Adv. Mater.* **2000**, *12*, 1403–1419.
- (12) Asefa, T.; Lennox, R. B. *Chem. Mater.* **2005**, *17*, 2481–2483.
- (13) (a) Tian, N.; Zhou, Z.-Y.; Sun, S.-G.; Ding, Y.; Wang, Z.-L. *Science* **2007**, *316*, 732–735. (b) Wiley, B.; Sun, Y.; Mayers, B.; Xia, Y. *Chem. Eur. J.* **2005**, *11*, 454–463.
- (14) Sun, J.; Ma, D.; Zhang, H.; Liu, X.; Han, X.; Bao, X.; Weinberg, G.; Pfänder, N.; Su, D. *J. Am. Chem. Soc.* **2006**, *128*, 15756–15764.
- (15) (a) Lim, M. H.; Blanford, C. F.; Stein, A. *J. Am. Chem. Soc.* **1997**, *119*, 4090–4091. (b) Stein, A.; Melde, B. J.; Schroden, R. C. *Adv. Mater.* **2000**, *12*, 1403–1419. (c) Lim, M. H.; Stein, A. *Chem. Mater.* **1999**, *11*, 3285–3295.
- (16) Margolese, D.; Melero, J. A.; Christiansen, S. C.; Chmelka, B. F.; Stucky, G. D. *Chem. Mater.* **2000**, *12*, 2448–2459. (b) Wang, X.; Lin, K. S. K.; Chan, J. C. C.; Cheng, S. J. *Phys. Chem. B* **2005**, *109*, 1763–1769. (c) Fowler, C. E.; Mann, S.; Lebeau, B. *Chem. Commun.* **1998**, 1825–1526.
- (17) (a) Möller, K.; Bein, T. *Chem. Mater.* **1998**, *10*, 2950–2963. (b) Fryxell, G. E.; Liu, J.; Hauser, T. A.; Nie, Z.; Ferris, K. F.; Mattigod, S.; Meiling, G.; Hallen, R. T. *Chem. Mater.* **1999**, *11*, 2148–2154.
- (18) (a) Asefa, T.; MacLachlan, M. J.; Coombs, N.; Ozin, G. A. *Nature* **1999**, *402*, 867–871. (b) Holland, B. T.; Blanford, C. F.; Stein, A. *Chem. Mater.* **1999**, *11*, 3302–3308. (c) Inagaki, S.; Guan, S.; Fukushima, Y.; Ohsuna, T.; Terasaki, O. *J. Am. Chem. Soc.* **1999**, *121*, 9611–9614.
- (19) (a) Asefa, T.; Kruk, M.; MacLachlan, M. J.; Coombs, N.; Grondev, H.; Jaroniec, M.; Ozin, G. A. *J. Am. Chem. Soc.* **2001**, *123*, 8520–8530. (b) Inagaki, S.; Guan, S.; Ohsuna, T.; Terasaki, O. *Nature* **2002**, *416*, 304–307. (c) Yang, Q.; Kapoor, M. P.; Inagaki, S. *J. Am. Chem. Soc.* **2002**, *124*, 9694–9695. (d) Hunks, W. J.; Ozin, G. A. *J. Mater. Chem.* **2005**, *15*, 3716–3724. (e) Yoshina-Ishii, C.; Asefa, T.; Coombs, N.; MacLachlan, M. J.; Ozin, G. A. *Chem. Commun.* **1999**, 2539–2540. (f) Whitall, W.; Asefa, T.; Ozin, G. A. *Adv. Funct. Mater.* **2005**, *15*, 1696–1702.
- (20) (a) Garcia, N.; Benito, E.; Guzman, J.; Tiemblo, P. *J. Am. Chem. Soc.* **2007**, *129*, 5052–5060. (b) Zapilko, C.; Liang, Y.-C.; Nerdal, W.; Anwender, R. *Chem. Eur. J.* **2007**, *13*, 3169–3176.
- (21) (a) Liu, J.; Feng, X. D.; Fryxell, G. E.; Wang, L.-Q.; Kim, A.-Y.; Gong, M. L. *Adv. Mater.* **1998**, *10*, 161–165. (b) Shylesh, S.; Singh, A. P. *J. Catal.* **2006**, *244*, 52–64. (c) Demicheli, G.; Maggi, R.; Mazzacani, A.; Righi, P.; Sartori, G.; Bigi, F. *Tetrahedron Lett.* **2001**, *42*, 2401–2403. (d) Hicks, J. C.; Dabestani, R.; Buchanan, A. C.; Jones, C. W. *Chem. Mater.* **2006**, *18*, 5022–5032. (e) Fajula, F.; Brunel, D. *Microporous Mesoporous Mater.* **2001**, *48*, 119–125.
- (22) Sharma, K. K.; Asefa, T. *Angew. Chem., Int. Ed.* **2007**, *46*, 2879–2882.
- (23) Kanai, M.; Kato, N.; Ichikawa, E.; Shibasaki, M. *Synlett* **2005**, 1491–1508.
- (24) Brunel, D.; Blanc, A. C.; Galarneau, A.; Fajula, F. *Catal. Today* **2002**, *73*, 139–152.
- (25) Cauvel, A.; Renard, G.; Brunel, D. *J. Org. Chem.* **1997**, *62*, 749–751.
- (26) (a) Han, L.; Ruan, J.; Li, Y.; Terasaki, O.; Che, S. *Chem. Mater.* **2007**, *19*, 2860–2867. (b) Huh, S.; Chen, H.-T.; Wiench, J. W.; Pruski, M.; Lin, V. S.-Y. *Angew. Chem., Int. Ed.* **2005**, *44*, 1826–1830. (c) Maeki-Arvela, P.; Kumar, N.; Kubicka, D.; Nasir, A.; Heikkilä, T.; Lehto, V.-P.; Sjöholm, R.; Salmi, T.; Murzin, D. Y. *J. Mol. Catal. A* **2005**, *240*, 72–81. (d) Huang, S.-J.; Huh, S.; Lo, P.-S.; Liu, S.-H.; Lin, V. S.-Y.; Liu, S.-B. *Phys. Chem. Chem. Phys.* **2005**, *7*, 3080–3087.
- (27) (a) Carter, P.; Wells, J. A. *Nature* **1988**, *332*, 564–568. (b) Bass, J. D.; Solovoyov, A.; Pascall, A. J.; Katz, A. J. *J. Am. Chem. Soc.* **2006**, *128*, 3737–3747. (c) Adams, R. D. *J. Organomet. Chem.* **2000**, *600*, 1–6.
- (28) (a) Topf, M.; Sandala, G. M.; Smith, D. M.; Schofield, C. J.; Easton, C. J.; Radom, L. *J. Am. Chem. Soc.* **2004**, *126*, 9932–9933. (b) Muller, R.; Debler, E. W.; Steinmann, M.; Seebeck, F. P.; Wilson, I. A.; Hilvert, D. *J. Am. Chem. Soc.* **2007**, *129*, 460–461. (c) Pereira, M. P.; Brown, E. D. *Biochemistry* **2004**, *43*, 11802–11812. (d) Jakopitsch, C.; Droghetti, E.; Schmuckenschlager, F.; Furtmüller, P. G.; Smulevich, G.; Obinger, C. *J. Biol. Chem.* **2005**, *280*, 42411–42422. (e) Wall, M.; Shim, J. H.; Benkovic, S. J. *Biochemistry* **2000**, *39*, 11303–11311.
- (29) (a) Jeong, N.; Seo, S. D.; Shin, J. Y. *J. Am. Chem. Soc.* **2000**, *122*, 10220–10221. (b) Hastoy, G.; Guillon, E.; Martens, J. *Stud. Surf. Sci. Catal.* **2005**, *158*, 1359–1366. (c) Aggarwal, V. K.; Bell, L.; Coogan, M. P. *J. Chem. Soc., Perkin Trans.* **1998**, *1*, 2037–2042.

Scheme 1. Synthesis of Aminopropyl-Functionalized Mesoporous Materials by Grafting Amino-organosilane in Various Solvents

groups.^{22,30} The distance between the two or more functional (catalytic) groups or the degree of their site-isolation is often crucial for these catalytic processes to yield the desired products effectively or efficiently.³¹ However, the determination of the degree of site-isolation of the functional groups, which is also essential to understand the mechanisms involved in the catalytic processes in these systems and to further design other efficient solid catalysts, has often been challenging.³² Furthermore, although methods such as titration,³³ fluorescence spectroscopy,^{27b,32} and solid-state NMR spectroscopy³⁴ have been used for the determination of distances between functional groups on solid substrates, they often involve expensive instruments and lengthy experimental procedures. For instance, by anchoring 4-pyrene-carboxylic acid fluorophores onto amine-functionalized mesoporous materials, Hicks et al. have determined the relative distances between the amine groups on mesoporous materials.^{32a} The fluorophores gave either monomer or excimer fluorescence, depending on the distances between the amine groups onto which they were anchored. Corriu's group used lanthanide ion-based fluorescence to determine the degree of site-isolation of crown ether-functionalized materials.^{32b} The titration of amides on proteins by acids has also been used to estimate distances between amino acids, since not all closely spaced amino acids undergo the acid–base reactions.³³ Similarly, a “Biuret” test,³⁵ which has long been used for analysis of amino acid concentration in body fluid, employs titration of proteins with Cu^{2+} to give characteristic color, electronic spectra, and λ_{max} depending on the number of closely spaced amides on the proteins.

Here, we report that the polarity and dielectric constants of solvents used for grafting organosilanes on mesoporous materials strongly affect the concentration of grafted organic groups, the degree of their site-isolation and distribution, and the catalytic properties of the resulting materials. We also report here a new simple colorimetric method for elucidating the degree of site-isolation of the organoamine groups on the materials. The study was carried out by grafting 3-aminopropyl, *N*-(2-aminoethyl)-

3-aminopropyl, 3-mercaptopropyl, 2-cyanoethyl, and methyl groups, which are among the most common types of organic groups grafted onto mesoporous silica (MCM-41).³⁶ The grafting of these functional groups onto MCM-41 was done under reflux for 6 h in various polar-protic, polar-aprotic, and nonpolar solvents by using (3-aminopropyl)trimethoxysilane, *N*-(2-aminoethyl)-(3-aminopropyl)triethoxysilane, (3-mercaptopropyl)trimethoxysilane, (2-cyanoethyl)trimethoxysilane, and methyltriethoxysilane, respectively (Scheme 1). The relative population of the organic groups, the structure, and the catalytic properties of the 3-aminopropyl-functionalized materials for the Henry (nitroaldol condensation) reaction³⁷ were found to strongly depend on the polarity and dielectric constant of the solvents. The colorimetric method for elucidation of the site-isolation of the functional groups relied on the different complexes that Cu^{2+} ions form with different distributions of the organoamines grafted on the MCM-41 with various solvents and the characteristic colors and absorption maxima (λ_{max}) on the electronic spectrum of the resulting materials. The colors and the λ_{max} were then used to characterize the degree of site-isolation of the organoamines. For instance, the monoamine- and diamine-functionalized samples grafted in methanol resulted in pale blue and light purple colors and λ_{max} at ~ 720 and 650 nm, respectively. These indicated the presence of CuNO_5 and CuN_2O_4 structures, respectively, and the presence of site-isolated organoamines in methanol grafting. The monoamine and diamine samples grafted in toluene resulted in purple and deep purple colors and absorption maxima at ~ 630 and 590 nm, respectively. These indicated the presence of CuN_2O_4 and CuN_4O_2 structures, respectively, and the presence of closely spaced organoamines in samples grafted in toluene. Samples grafted in isopropanol gave colors and λ_{max} intermediate between those of samples grafted in toluene and methanol.

(30) McKittrick, M. W.; Jones, C. W. *J. Am. Chem. Soc.* **2004**, *126*, 3052–3053.

(31) Okino, T.; Hoashi, Y.; Furukawa, T.; Xu, X. N.; Takemoto, Y. *J. Am. Chem. Soc.* **2005**, *127*, 119–125.

(32) (a) Hicks, J. C.; Dabestani, R.; Buchanan, A. C.; Jones, C. W. *Chem. Mater.* **2006**, *18*, 5022–5032. (b) Mouawia, R.; Mehdi, A.; Reyé, C.; Corriu, R. J. P. *New J. Chem.* **2006**, *30*, 1077–1082.

(33) May, F. E. B.; Church, S. T.; Major, S.; Westley, B. R. *Biochemistry* **2003**, *42*, 8250–8259.

(34) (a) Hashidzume, A.; Harada, A. *Polymer* **2005**, *46*, 1609–1616. (b) Azurmendi, H. F.; Wang, S. C.; Massiah, M. A.; Poelarends, G. J.; Whitman, C. P.; Mildvan, A. S. *Biochemistry* **2004**, *43*, 4082–4091.

(35) Drochioiu, G.; Damoc, N. E.; Przybylski, M. *Talanta* **2006**, *69*, 556–564.

(36) (a) Shimizu, K.; Hayashi, E.; Inokuchi, T.; Kodama, T.; Hagiwara, H.; Kitayama, Y. *Tetrahedron Lett.* **2002**, *43*, 9073–9075. (b) Wang, X.; Lin, K. S. K.; Chan, J. C. C.; Cheng, S. *Chem. Commun.* **2004**, 2762–2763. (c) Clark, J. *Acc. Chem. Res.* **2002**, *35*, 791–797. (d) Kruk, M.; Asefa, T.; Jaroniec, M.; Ozin, G. A. *Stud. Surf. Sci. Catal.* **2002**, *141*, 197–204. (e) Yang, H.-Q.; Zhang, G.-Y.; Hong, X.-L.; Zhu, Y.-Y. *Microporous Mesoporous Mater.* **2004**, *68*, 119–125. (f) Matheron, M.; Bourgeois, A.; Gacoin, T.; Brunet-Bruneau, A.; Albouy, P. A.; Boilot, J. P.; Biteau, J.; Lacan, P. *Thin Solid Films* **2006**, *495*, 175–179. (g) Wang, X.; Lin, K. S. K.; Chan, J. C. C.; Cheng, S. *J. Phys. Chem. B* **2005**, *109*, 1763–1769. (h) Choudary, B. M.; Kantam, M. L.; Srekanth, P.; Bandopadhyay, T. Figueras, F.; Tuel, A. *J. Mol. Catal. A* **1999**, *142*, 361–365.

(37) (a) Luzzio, F. A. *Tetrahedron* **2001**, *57*, 915–945. (b) Palomo, C.; Oiarbide, M.; Mielgo, A. *Angew. Chem., Int. Ed.* **2004**, *43*, 5442–5444. (c) Yamada, Y. M. A.; Yoshikawa, N.; Sasai, H.; Shibasaki, M. *Angew. Chem., Int. Ed.* **1997**, *36*, 1871–1873. (d) Trost, B. M.; Itoh, H.; Silcoff, E. R. *J. Am. Chem. Soc.* **2001**, *123*, 3367–3368. (e) Rosini, G.; Ballini, R. *Synthesis* **1988**, 833–847.

2. Experimental Section

Materials and Reagents. *p*-Hydroxybenzaldehyde, cetyltrimethylammonium bromide, tetraethylorthosilicate, (2-cyanoethyl)trimethoxysilane (CETS), copper sulfate, nitromethane, and formamide were obtained from Sigma-Aldrich, and they were used without further purification. (3-Aminopropyl)trimethoxysilane (APTS), *N*-(2-aminoethyl)-(3-aminopropyl)triethoxysilane (AAPTS), methyltriethoxysilane (MTS), and (3-mercaptopropyl)trimethoxysilane (MPTS) were purchased from Gelest, Inc. Anhydrous methanol and isopropanol were received from Pharmco-AAEPR. Acetic acid, isopropanol, acetone, chloroform, ethyl acetate, toluene, acetonitrile, *N,N*-dimethylformamide (DMF), and dimethyl sulfoxide (DMSO) were obtained from Fisher Scientific.

Synthesis of Organic-Grafted Mesoporous Materials. A mesoporous material, MCM-41, was synthesized by two methods as reported previously.^{18,19,22,38} Both synthesis methods of MCM-41, namely by using NH₄OH and aging for 2 days at 80 °C^{18,19} as well as by using NaOH and stirring for 2 h at 80 °C,^{22,38} gave similar results. The MCM-41 was kept in an oven at 80 °C to remove physisorbed water prior to grafting. For example, 500 mg of the dry MCM-41 was stirred with excess APTS (3.68 mmol) in ~250 mL of the solvent under reflux (or the boiling point of the solvent except for DMF, toluene, and DMSO, where 80 °C was used) for 6 h. The solvents used were as follow: (1) polar-protic solvents, isopropanol, ethanol, methanol, and formamide; (2) dipolar-aprotic solvents, ethyl acetate, tetrahydrofuran (THF), acetone, DMF, DMSO, and acetonitrile; and (3) nonpolar solvents, toluene and chloroform. After the grafting of the organosilane, the solution was filtered and the solid material was washed with ethanol and then dried in air.

Similarly, 3.68 mmol of MPTS, MTS, or AAPTS was grafted on MCM-41 following the same procedure as above with isopropanol and toluene as solvents.

Synthesis of Organoamine-Grafted Mesoporous Materials and Cu²⁺ Complexes. The 3-aminopropyl (AP)-functionalized samples in methanol, isopropanol, and toluene above were labeled as AP-M, AP-I, and AP-T, respectively, while the *N*-(2-aminoethyl)-3-aminopropyl (AAP)-functionalized samples in methanol, isopropanol, and toluene were labeled as AAP-M, AAP-I, and AAP-T, respectively. Four additional samples were prepared by taking the elemental analysis results of these samples into account. The grafting of MCM-41 with excess amino-organosilanes in methanol and isopropanol resulted in ~1 and 2 mmol of organoamine group per unit gram of sample, whereas the corresponding grafting in toluene resulted in ~3 mmol of organoamine per unit gram of sample (see Results and Discussion below). To prepare samples in toluene but by using the same amount (millimoles) of amino-organosilanes as that grafted by methanol or isopropanol, 500 mg of MCM-41 sample was stirred with 1 or 2 mmol of APTS or AAPTS, respectively, in toluene by following the same procedure as above. The resulting materials from APTS were labeled as AP-MT and AP-IT, respectively, whereas those from AAPTS were denoted as AAP-MT and AAP-IT, respectively. Amino-organosilanes in toluene have a stronger tendency to graft onto the mesoporous silica surface,²² although in aggregates.^{32a} Thus, these samples are expected to have aggregated organoamine groups despite the low concentration of organosilanes used and despite the lower number of grafting resulting from the latter, compared to if excess organosilane in toluene was used. For instance, AP-M and AP-MT would have similar percentages of grafted organoamine groups but different distribution or degree of site-isolation. The AP-M is expected to have site-isolated groups, while the AP-MT is expected to have aggregated groups.

Twenty-milligram portions of each of the amine-functionalized samples (AP-M, AP-I, AP-T, AP-MT, AP-IT, AAP-M, AAP-I, AAP-T, AAP-MT, or AAP-IT) were stirred in 5 mL of 0.001 M, 5 mL of

0.002 M, 5 mL of 0.004 M, 5 mL of 0.008 M and 5 mL of 0.016 M aqueous Cu²⁺ solution. The samples were sonicated for 5 min and then kept under static conditions for 1 h. The solution was centrifuged, the supernatant was separated, and the precipitate was quickly washed with 5 mL of ethanol and allowed to dry under ambient conditions. The resulting samples from AP-MT, for instance, with the aforementioned different concentrations of Cu²⁺ were labeled as AP-MT1, AP-MT2, AP-MT3, AP-MT4, and AP-MT5, respectively. The other samples were also labeled with the same trend. Additional samples were prepared by stirring the AP-M, AP-I, and AP-T in excess Cu²⁺ solution (20 mL, 0.05 M). The latter solutions were kept under static conditions for 12 h. They were then centrifuged, the supernatant was separated, and the precipitate was washed with 5 mL water and allowed to dry under ambient conditions. The resulting samples were denoted as AP-M-E, AP-I-E, and AP-T-E.

Control Samples. Control samples in solution phase were prepared by mixing APTS and Cu²⁺ solution with APTS:Cu²⁺ mole ratios of 8:1, 4:1, 2:1, 1:1, and 1:2 in 5 mL of water. Each solution was sonicated for 5 min and then kept for 1 h without sonication. Similarly, AAPTS was mixed with Cu²⁺ solution in AAPTS:Cu²⁺ mole ratios of 4:1, 2:1, 1:1, 1:2, and 1:4 in 5 mL of water. Some of the APTS/Cu²⁺ solutions were observed to give a precipitate, due to the hydrolysis and condensation of the alkoxysilyl groups. The resulting solutions and precipitates (in the cases of precipitate formation) were characterized by UV-vis absorption and reflectance spectroscopy (see Results and Discussion below).

Henry (Nitroaldol Condensation) Reaction. The Henry reaction was done as reported before.²² Typically, 21 mg of the AP-functionalized mesoporous samples was added into a mixture of 122 mg (1 mmol) of *p*-hydroxybenzaldehyde and 10 mL of nitromethane. The reaction mixture was stirred at 90 °C under nitrogen, and aliquots of the solution were taken with a filter syringe and characterized by solution ¹H NMR spectroscopy and GC-MS over the course of the reaction. The percent yield and conversion were determined by using ¹H NMR spectra measured in deuterated acetone.

Instrumentation. The powder X-ray diffraction (XRD) was measured using a Scintag powder diffractometer. The solid-state ¹³C (75.5 MHz) and ²⁹Si (59.6 MHz) NMR spectra were acquired on a Bruker AVANCE 300 spectrometer. For ¹³C CP-MAS NMR experiments, we employed a 7.0 kHz spin rate, 5 s recycle delay, 1 ms contact time, $\pi/2$ pulse width of 5.2 μ s, and 1000–3000 scans using two-pulse phase modulation (TPPM) ¹H decoupling. For the ²⁹Si CP-MAS NMR experiments, we employed a 7.0 kHz spin rate, 10 s recycle delay, 10 ms contact time, $\pi/2$ pulse width of 5.6 μ s, and 256–1024 scans using TPPM ¹H decoupling. The ²⁹Si MAS NMR experiments were done with a 7.0 kHz spin rate, 100 s recycle delay, $\pi/6$ pulse width of 1.9 μ s, and 700–4000 scans using high-power continuous-wave ¹H decoupling. The solution ¹H NMR was measured by using a Bruker DPX-300 NMR spectrometer. The BET gas adsorptions were measured with Micromeritics ASAP 2020 and Micromeritics Tristar 3000 volumetric adsorption analyzers at 77 K by following previously reported procedures.³⁹ The Cu²⁺-complexed powder samples and control samples were characterized visually and by diffuse reflectance or absorption UV-vis spectroscopy (LAMBDA-950, Perkin Elmer). For the UV-vis reflectance measurements, the solid powder samples were ground into fine powder and then kept between two quartz plates, each 1 mm thick. The samples were made to cover one quartz plate as uniformly and completely as possible. Another quartz plate was then put on top of the samples and rubbed slowly to form a smooth, flat sandwiched sample before being mounted for UV-vis measurements. The UV-vis absorption spectra of the control samples (solutions) were measured in quartz cuvettes. The transmission electron microscopy

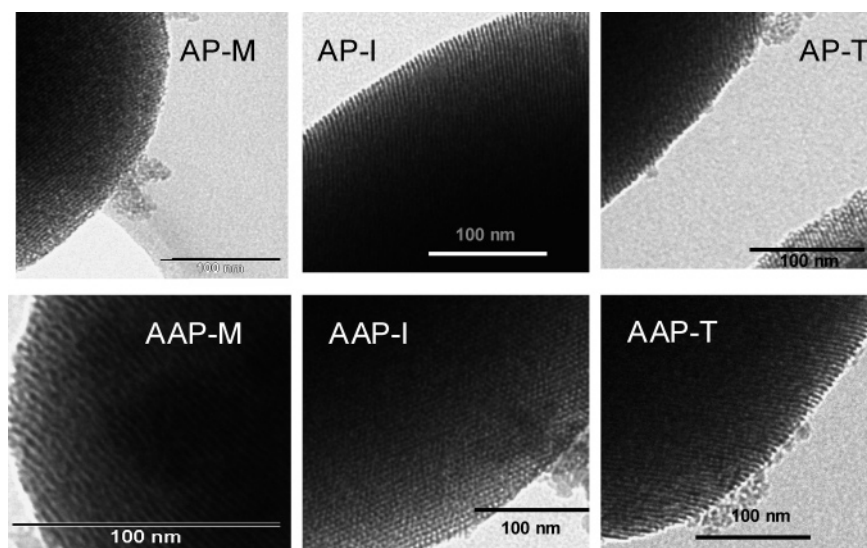
(38) Seong, H.; Chen, H.-T.; Wiench, J. W.; Pruski, M.; Lin, V. S.-Y. *Angew. Chem., Int. Ed.* **2005**, *44*, 1826–1830.

(39) (a) Kruk, M.; Asefa, T.; Coombs, N.; Jaroniec, M.; Ozin, G. A. *J. Mater. Chem.* **2002**, *12*, 3452–3457. (b) Kruk, M.; Jaroniec, M. *Chem. Mater.* **2001**, *13*, 3169–3183.

Table 1. Surface Areas, Compositions, and Properties of 3-Aminopropyl-Functionalized Mesoporous Materials Obtained by Grafting MCM-41 in Various Solvents

solvent	dielectric constant, ϵ	wt % N, elemental analysis	% T ^a	wt % (100–600 °C)	surface area (m ² /g)	catalytic efficiency (% yield in 12 min) ^b
Polar-Protic Solvents						
isopropanol	18	2.92	11.7	12.0	902 (±7)	92
ethanol	24	1.71	7.2	12.5	905 (±3)	89
methanol	33	1.39	6.8	8.0	864 (±3)	72
formamide	84	2.90 ^c	na	na	659 (±4)	5
Nonpolar and Dipolar-Aprotic Solvents						
toluene	2.4	3.82	23.4	17.8	259 (±5)	42
chloroform	4.8	3.24	22.0	15.2	628 (±7)	99
ethyl acetate	6.0	3.55	24.0	18.5	153 (±4)	28
THF	7.5	3.75	17.1	15.4	293 (±7)	36
acetone	21	3.38	16.6	13.5	617 (±7)	94
DMF	38	3.82 ^c	20.4	17.5	501 (±11)	58
acetonitrile	38	2.52	18.6	14.0	618 (±6)	83
DMSO	47	3.47	17.8	13.8	620 (±11)	99

^a % T is the percentage of aminopropylsilica $\{(\text{OH})_x\text{O}_y\text{Si}-(\text{CH}_2)_3\text{NH}_2\}$ obtained from the integration of peaks in the ²⁹Si MAS NMR spectra. ^b The yield of the reaction between 1 mmol of *p*-hydroxybenzaldehyde and 10 mL of nitromethane at 15 min of reaction time for 21 mg of catalyst. ^c The nitrogen content in these samples may have also been contributed by the solvents themselves, which physisorb inside the channels of the functionalized mesoporous samples and which are hard to completely remove due to their high boiling points. This was also consistent with the results observed on thermogravimetric analysis (TGA) traces (see below and Figure S2).

**Figure 1.** Representative transmission electron microscopy (TEM) images of MCM-41 and of some representative 3-aminopropyl (AP)- and *N*-(2-aminoethyl)-(3-aminopropyl)triethoxysilane (AAP)-grafted samples in various solvents.

(TEM) images were taken by using an FEI Tecnai G-20 TEM/STEM microscope working at 120 keV accelerating voltage.

3. Results and Discussion

A series of organic-functionalized mesoporous materials containing different concentrations and distributions of AP, AAP, 3-mercaptopropyl, 2-cyanoethyl, or methyl groups were synthesized. This was carried out by grafting the corresponding organosilanes onto mesoporous silica (MCM-41) under reflux in various polar-protic, dipolar-protic, and nonpolar solvents (Scheme 1). Briefly, the organosilane was refluxed with MCM-41 in the solvent under nitrogen for 6 h (Table 1). The MCM-41 was synthesized as reported previously,^{22,38,40} and it was kept in an oven to remove most of its physisorbed water prior to grafting. The relative populations of the grafted organic groups and the structures and catalytic properties of the materials were then investigated.

The TEM images (Figure 1) and the XRD patterns (Figure 2) exhibited that all the functionalized samples had highly ordered mesostructures with unit cell dimensions of ~ 44 – 45 Å (Figure 1). The TEM and XRD results also revealed that the grafting of organosilanes on the MCM-41 sample in various polar-protic, dipolar-protic, and nonpolar solvents did not cause major structural differences between the samples. This was further corroborated by N₂ gas adsorption, which showed a type IV isotherm and a single peak on the pore size distribution plot for all the samples, which are indicative of ordered mesoporous structures (Figure S1). However, the surface areas of the materials varied from 150 to 900 m²/g, while the average pore sizes varied between 27 and 34 Å (Table 1 and Table S1), depending on the solvent used or the percentage of organofunctional groups grafted (see below). The samples with higher percentage of grafted organic groups, as corroborated by elemental analysis (see below), often showed lower surface areas (Figures 3 and 4), as expected.⁴¹ It is worth mentioning that a few of the samples did not strictly follow this trend due to

(40) Huh, S.; Chen, H.-T.; Wiench, J. W.; Pruski, M.; Lin, V. S.-Y. *J. Am. Chem. Soc.* **2004**, *126*, 1010–1011.

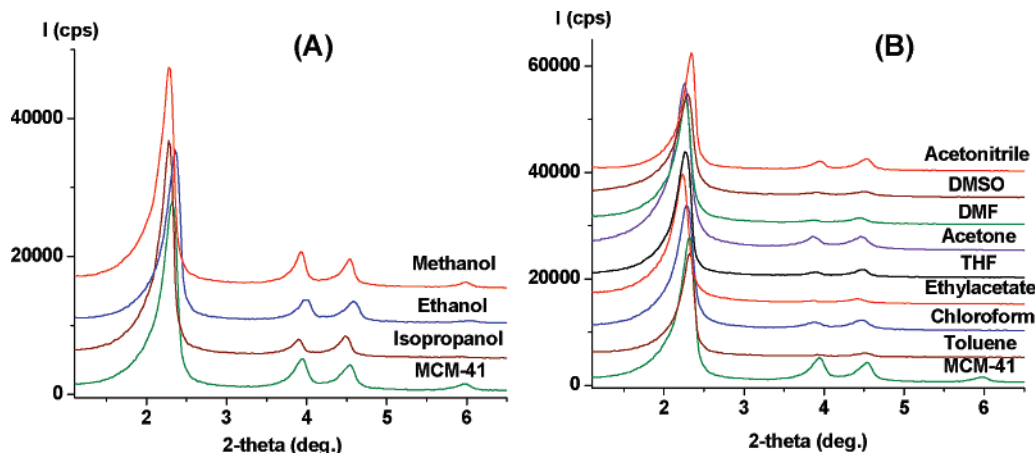


Figure 2. (A) Powder X-ray diffraction (XRD) patterns of MCM-41 and AP-grafted samples synthesized in polar-protic solvent. (B) XRD patterns of AP-grafted samples synthesized in various nonpolar and dipolar-aprotic solvents.

differences in the degree of aggregation of the grafted groups in some solvents and the percentage of aminosilanes adsorbed on the mesoporous silica by a hydrogen-bonding interaction between the aminosilanes and the surface silanols in these materials. For instance, samples grafted in toluene, THF, and ethyl acetate have percentages of grafting comparable to those of samples grafted in chloroform, acetone, and DMF. However, the two series of samples exhibited a significant difference in surface area because the former have produced more aggregated grafted groups while the latter have more spatially isolated grafted groups. The degree of aggregation or spatial separation was established colorimetrically with Cu^{2+} complexes (see below). Furthermore, the samples grafted in toluene, THF, and ethyl acetate also showed the presence of some adsorbed aminosilanes, which was proved by washing the samples thoroughly with ethanol and water and measuring the surface areas and the percentage of grafted groups for the samples afterward. The samples grafted in toluene, THF, and ethyl acetate showed a slight increase in surface area and a slight decrease in weight-percent N (organoamine) after washing (see Table S2 and Figure S1E). Strong adsorption of aminosilanes on the silica surface was possible due to strong hydrogen-bonding, as reported previously for silica gel materials.⁴²

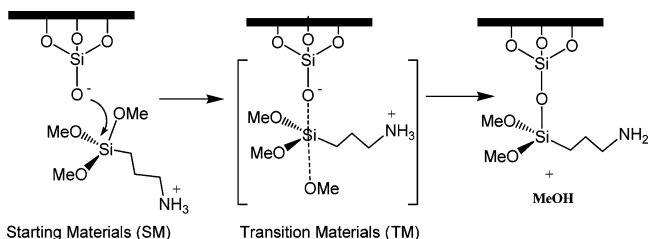
The percentage of the grafted AP groups was determined from elemental analysis (Tables 1 and S2).⁴³ The elemental analysis results were further corroborated by the weight loss in the range of 150–600 °C on thermogravimetric analysis (TGA) traces (Figure S2) and by quantitative solid-state ^{29}Si MAS NMR spectroscopy (Table 1 and Figures S3–S5).⁴⁴ The results indicated that samples grafted in polar-protic solvents have lower

Table 2. Surface Areas and Compositions of 3-Mercaptopropyl- and 2-Cyanoethyl-Functionalized Mesoporous Materials by Grafting MPTS and CETS in Polar and Nonpolar Solvents

organosilane	solvent	dielectric constant, ϵ	wt % S, elemental analysis	wt % N, elemental analysis	surface area (m^2/g)
MPTS	isopropanol	18	2.18 ^a		762
MPTS	toluene	2.4	4.81 ^a		633
CETS	isopropanol	18		0.54	697
CETS	toluene	2.4		2.56	690

^a It is worth noting that the atomic mass of sulfur is more than twice that of nitrogen. After considering this fact, we find that the percentage of grafting of MPTS indeed is much lower than that of APTS in all the solvents. This result was further confirmed by ^{29}Si solid-state NMR spectroscopy (see Figure S6).

Scheme 2. Grafting of Organosilane on Silica Surface via an $\text{S}_{\text{N}}2$ Mechanism



percentages of AP groups compared to those grafted in nonpolar and dipolar-aprotic solvents. On the other hand, the grafting of hydrophobic 3-mercaptopropyl groups by using MPTS in ethanol or toluene resulted in significantly lower percentage of grafted groups compared to corresponding AP-grafted samples, as indicated by both elemental analysis and ^{29}Si MAS NMR (Table 2 and Figure S6).

The relationship between solvent polarity and grafting concentration of organosilanes (Table 1) was explained on the basis of the effects of solvation and dielectric properties of solvents on $\text{S}_{\text{N}}2$ reactions on silicon atoms,⁴⁵ similar to $\text{S}_{\text{N}}2$ reactions on carbon atoms (Scheme 2). Solvation of reactants is known to affect reaction rates and mechanisms in organic reactions.⁴⁶ To arrive at the solvation-based explanations, we first made the following reasonable assumptions: (1) All the solvents were assumed to have no significant differences in diffusion from the liquid to the solid phase (the mesopores).

(41) Grafting of organic groups on mesoporous materials is often accompanied with loss of surface areas. For example, see: (a) Feng, X.; Fryxell, G. E.; Wang, L. Q.; Kim, A. Y.; Liu, J.; Kemner, K. M. *Science* **1997**, *276*, 923–926. (b) Sakthivel, A.; Abrantes, M.; Chiang, A. S. T.; Kuhn, F. E. *J. Organomet. Chem.* **2006**, *691*, 1007–1011. (c) Gutierrez, O. Y.; Fuentes, G. A.; Salcedo, C.; Klimova, T. *Catal. Today* **2006**, *116*, 485–497. (d) Abrantes, M.; Gago, S.; Valente, A. A.; Pillinger, M.; Goncalves, I. S.; Santos, T. M.; Rocha, J.; Romao, C. C. *Eur. J. Inorg. Chem.* **2004**, 4914–4920.

(42) Engelhardt, H.; Orth, P. *J. Liq. Chromatogr.* **1987**, *10*, 1999–2022.

(43) Elemental analysis is commonly used for quantifying the percentages of grafted organic and organometallic complexes on mesoporous materials. For example, see: Wang, X.; Lin, K. S. K.; Chan, J. C. C.; Cheng, S. *Chem. Commun.* **2004**, 2762–2763.

(44) The percentage of the grafted groups from solid-state NMR is consistent with the elemental analysis and TGA results. However, the samples grafted with DMF and DMSO showed a slightly higher percentage of organoamine groups in the elemental analysis and TGA than in the NMR analysis due to some physisorbed DMF and DMSO in the samples.

(45) Corriu, R. J. P.; Guerin, C.; Henner, J. L.; Wang, Q. *Organometallics* **1991**, *10*, 3200–3205.

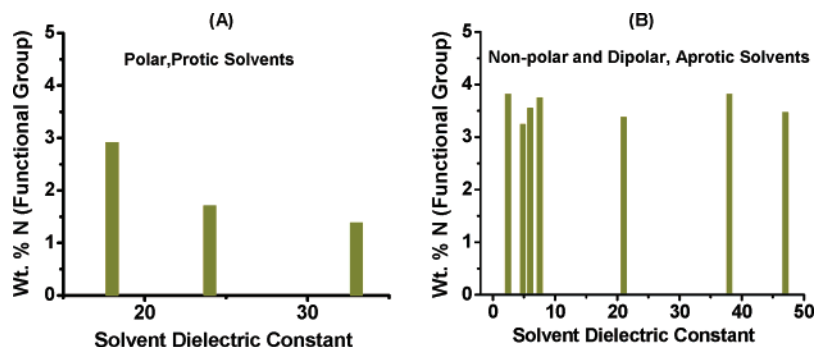


Figure 3. Weight-percent of N (percentage of grafted functional groups) versus solvent dielectric constant for samples grafted with (A) polar-protic solvents and (B) nonpolar and dipolar-aprotic solvents.

This assumption is made to simplify the arguments and is based on our observations that the samples sink in solvents immediately. To the best of our understanding, variations in diffusion would not be a decisive factor in determining the grafting concentration of the organosilanes on the mesoporous matrix. (2) The grafting reaction mechanism was assumed to follow an S_N2 attack of a nucleophile on the Si atom to give a five-membered transition state (TS) that is destabilized with respect to the starting materials due to the steric bulk of the methoxy or ethoxy substituent on the Si atom (Scheme 2). Hence, all the considerations that apply to the S_N2 attack at the carbon centers in terms of the polarity and solvation capability of the solvent also apply to nucleophilic substitution at the Si atom. This assumption is based also on a recently published article⁴⁷ and is contrary to the popular belief that nucleophilic substitutions at the Si atom goes through a stable five-membered TS; i.e., the reaction coordinate follows a potential energy well, which is true only for less bulky substituents such as hydrogen, methyl, and ethyl.⁴⁷ When the substituents around silicon become bulkier, such as methoxy and ethoxy groups, the potential energy well changes from a minimum to a central maximum. (3) The nucleophile attacking the Si atom is assumed to be a silanolate ($Si-O^-$ anion),⁴⁸ which is expected to be in an appreciable concentration due to the low isoelectronic point of silica, IEP ≈ 2.0 (although we can also safely assume the $Si-OH$ groups to be the nucleophile).⁴⁹ The silanolate anion is the active nucleophile even if present in a small concentration, because it is a stronger nucleophile than $Si-OH$, more so under the anhydrous conditions used for grafting, and hence would have a higher probability of attacking the Si atom. (4) The grafting concentration in a given time, at a given temperature, and for a given MCM-41 parent material is assumed to be a direct measure of the rate of reaction of the organosilane. With these four assumptions in mind, the solvents used in this work have been broadly classified into the following three categories: (a) polar-protic, (b) dipolar-aprotic, and (c) nonpolar. To understand the effects of the solvent, a general mechanism of the reaction taking place is shown in Scheme 2.

The reaction coordinate for the mechanism in Scheme 2 and the factors that lead to a change in reaction coordinate (as in ref 46) can be described as follows:

(1) Polar-protic solvents. These solvents solvate the reactants better than the TS because the charge in the starting materials (SM) gets dispersed in the TS (Scheme 2). It is also worth noting that the nucleophile undergoes solvation more than the organosilane. The solvation of the nucleophile leads to a significant decrease in its nucleophilicity or reactivity because of the

dominant solvent cage.⁵⁰ In terms of the energy profile, since the reactants get stabilized better than the TS, this leads to an increase in the activation energy (E_a) of the TS; consequently, the reaction rate is slowed. The increase in the E_a can also be thought of as the “extra” energy required to break the solvent cage before the nucleophile can attack the Si atom.

Further, among the polar-protic solvents, varying the dielectric constant also leads to a change in the energy profile. An increase in the dielectric constant leads to the stabilization of the reactants more than the TS due to localized charge in the SM. Thus, an increase in the dielectric constant decreases the reaction rate by increasing the E_a . Therefore, increases in the dielectric constant and the polarity of the polar-protic solvents favor an increase in the E_a of the reaction. This clearly explains the decrease in the percentage of organic groups grafted as the dielectric constant increases in the polar-protic solvents series (Table 1 and Figure 3). Thus, on going from isopropanol to methanol, the dielectric constant increases from 18 to 33, and concomitantly, the organic group grafting evaluated on the basis of wt % N decreases from 2.92 to 1.31 (Table 1 and Figure 3).

(2) Dipolar-aprotic solvents. In these solvents, the only stabilization which the nucleophile has is from the ion–dipole interactions, as H-bonding capacity is significantly low. Thus, compared to that observed with polar-protic solvents, the nucleophilicity is increased. A comparison of the energy profiles of the polar-protic and dipolar-aprotic solvents demonstrates that the stabilization of the SM is significant in the former and hence the activation energy is higher. Thus, dipolar-aprotic solvents have lower activation energies as compared to those of the polar-protic solvents. This leads to a faster reaction rate in the case of dipolar-aprotic solvents and hence greater organosilane

- (46) (a) Gao, J. L.; Garcia-Viloca, M.; Poulsen, T. D.; Mo, Y. R. *Adv. Phys. Org. Chem.* **2003**, *38*, 61–68. (b) Hayakawa, F.; Watanabe, S.; Shimizu, N.; Tsuno, Y. *Bull. Chem. Soc. Jpn.* **1993**, *66*, 153–157. (c) Bentley, T. W.; Dauschmidt, J. P.; Llewellyn, G.; Mayr, H. *J. Org. Chem.* **1992**, *57*, 2387–2392. (d) Pliego, J. R. *J. Mol. Catal. A* **2005**, *239*, 228–234.
- (47) Bento, A. P.; Bickelhaupt, F. M. *J. Org. Chem.* **2007**, *72*, 2201–2207.
- (48) (a) Corriu, R. J. P.; Leclercq, D. *Angew. Chem., Int. Ed.* **1996**, *35*, 1420–1436. (b) Walcarius, A.; Etienne, M.; Lebeau, B. *Chem. Mater.* **2003**, *15*, 2161–2173.
- (49) Silanols ($Si-OH$) could behave as a nucleophile the same way as H_2O behaves as a nucleophile (for example, see: Corriu, R. J. P.; Guerin, C.; Henner, J. L.; Wang, Q. *Organometallics* **1991**, *10*, 3200–3205), but the rate of nucleophilic attack by $Si-OH$ would be slower than that by $Si-O^-$. The latter is often produced in the presence of a basic solution in sol-gel reactions. Although aminopropyl groups are not strong enough to abstract protons from all the silanols, they are reported by Walcarius et al.^{48b} that they help the formation of a significant number of silanolate anions ($Si-O^-$) in amino-functionalized mesoporous materials.
- (50) Zeidan, R. K.; Hwang, S.-J.; Davis, M. E. *Angew. Chem., Int. Ed.* **2006**, *45*, 6332–6335.

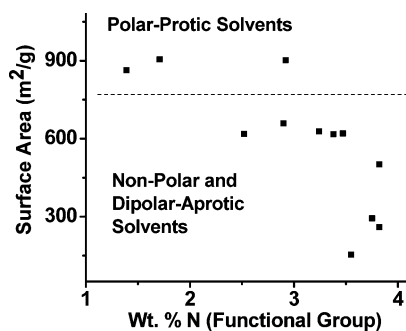


Figure 4. Surface area versus weight-percent N (percentage of grafted functional groups) for 3-aminopropyl (AP)-functionalized samples in various solvents.

grafting in a given time. The average loading in the polar-protic solvents is found to be 2.00 wt % N (based on isopropanol, ethanol, and methanol), while for the dipolar-protic solvents, it is 3.30 wt % N (for acetone, DMF, acetonitrile, and DMSO) (Table 1). This explains the higher grafting obtained in these solvents. Furthermore, a variation in the dielectric constant of the solvent again affects the activation energy in the same manner as in the polar-protic solvents; i.e., an increase in dielectric constant leads to an increase in E_a , leading to a decrease in the reaction rate and hence a decrease in the grafting concentration. This could be seen on comparing the results of DMF and DMSO.

The lower value of grafting or anomalous behavior obtained for acetone could be attributed to its formation of imine, which retards the reaction rate (because of the energy required to form the kinetically fast imines and also because the steric bulk of the molecule increases, leading to slower diffusion). The only result that this model fails to explain is that of the acetonitrile.

c) Nonpolar solvents. These solvents provide negligible solvation to the nucleophile but are apt at solvating the organosilane on account of the presence of alkoxy substituents in them. However, since the only solvation is through the van der Waals interaction or minimal ion–dipole interaction in the case of aminosilanes, this solvation contributes very little in changing the energy profile. But “destabilization” or less stabilization of the nucleophile in these solvents decreases the E_a markedly, and consequently, the reaction rate increases. This is reflected in a drastic increase in grafting concentration to an average of 3.51 wt % N (for ethyl acetate, THF, chloroform, and toluene) (Table 1 and Figure 3).

Among the solvents, the least polar solvents, such as toluene and chloroform, would provide maximum stabilization to the organosilane through solvation, leading to an increase in the activation energy and a decrease in the reaction rate; i.e., in nonpolar solvents, the effect of increasing the dielectric constant is just the reverse of what was observed in the other two types of solvents. Since now the organosilane is stabilized by a low-dielectric medium, increasing the dielectric constant of the medium would serve to increase the reaction rate by decreasing the activation energy, as observed in chloroform, ethyl acetate, and THF.

The trend in the relationship between the dielectric constant and the percentage of organic groups for APTS grafting could also be related to the hydrogen-bonding interactions between the amino-organosilane and the solvents. The strong hydrogen-bonding between amine groups of APTS and the polar-protic solvents^{21d} lowers the tendency of the amino-organosilane to go to the silanol groups to graft. Solvents with higher dielectric constant form stronger hydrogen-bonding interactions. The obtained trend in the percentage of organic groups was isopropanol > ethanol > methanol > formamide, and it confirmed that solvents with higher dielectric constant grafted fewer organic groups. This relationship between dielectric constant and percentage of organic group is not clear for the series of dipolar-protic solvents, as there is no direct correlation between hydrogen-bonding and dielectric constant for these solvents.

The efficiency of the AP-functionalized materials to catalyze the Henry reaction between *p*-hydroxybenzaldehyde and nitromethane also showed an interesting trend (Figure 5, Figure S7, and Table 1). For the polar-protic solvents used for grafting, the catalytic efficiency of the materials decreased in the order of isopropanol > ethanol > methanol > formamide. This is consistent with the concentrations of grafted organoamines. The sample grafted with isopropanol showed unprecedented catalytic efficiency, even compared to a catalyst we reported recently using ethanol.²² The sample grafted in isopropanol exhibited a slightly higher number of grafted organoamines compared to ethanol and methanol. Upon grafting in dipolar-protic solvents, the concentration of organoamines increased but the efficiency decreased, except in acetonitrile. Further, the sample grafted in acetone, which formed imines⁵¹ as observed from its obvious yellowish color, showed an exceptional higher yield in the series of solvents as well.⁵² We further found that samples that have higher surface areas also have higher catalytic efficiency.

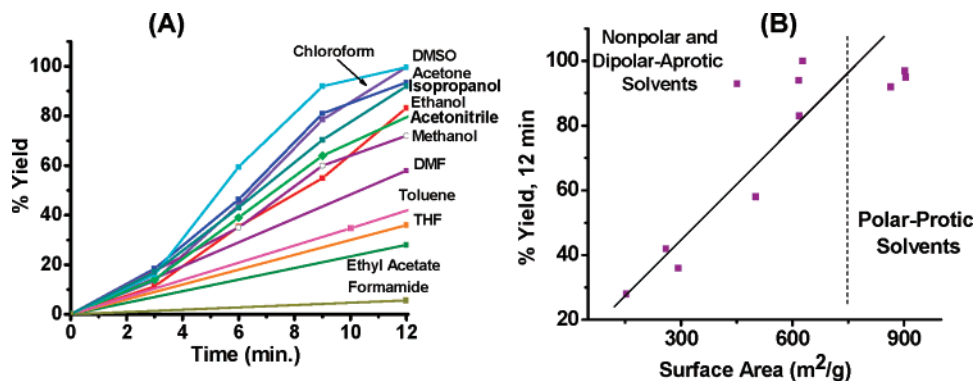


Figure 5. (A) Reaction yield versus time for the Henry reaction catalyzed by the aminopropyl-functionalized mesoporous materials grafted in various solvents. (B) Reaction yield after 12 min versus surface area of the materials.

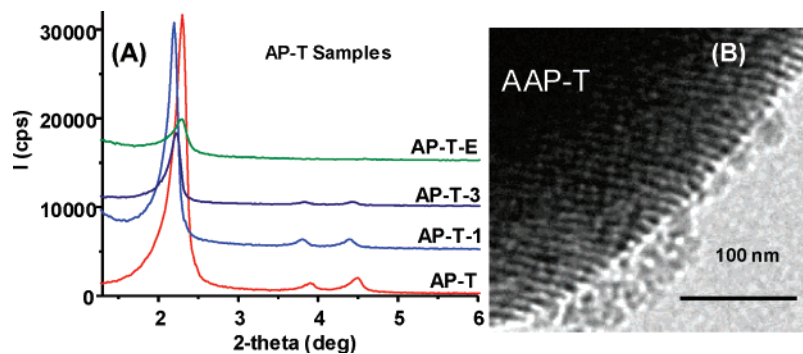


Figure 6. (A) XRD patterns of representative Cu^{2+} -complexed organoamine (AP)-functionalized samples. (B) TEM image of a representative Cu^{2+} -complexed organodiamine (AAP)-functionalized sample.

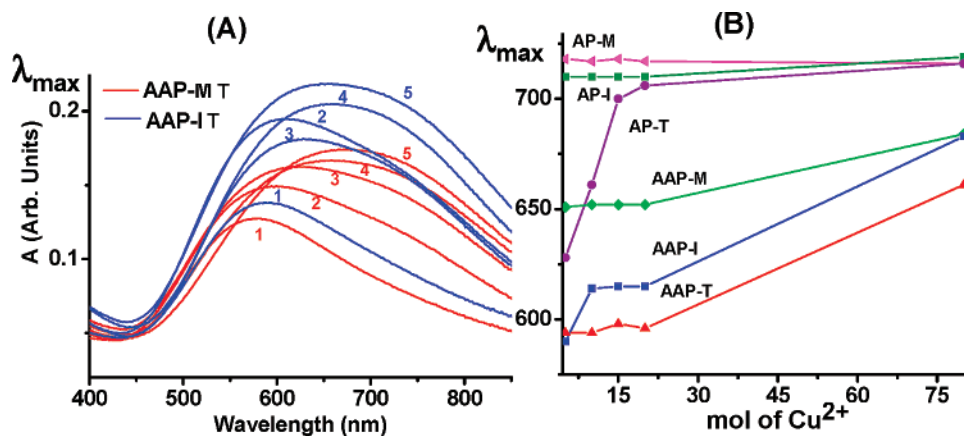


Figure 7. (A) Representative UV-vis reflectance spectra for Cu^{2+} -complexed organodiamine (AAP)-functionalized mesoporous samples. Spectra 1–5 are for samples with increasing concentrations of Cu^{2+} (see Table 2). (B) λ_{max} values of the metalated samples studied versus millimoles of $[\text{Cu}(\text{H}_2\text{O})_6]^{2+}$ used.

However, the differences in surface areas alone did not explain the observed differences in the catalytic efficiency. For instance, samples grafted in acetone and acetonitrile showed similar surface areas, but the former showed greater catalytic efficiency. These results clearly revealed that a combination of surface area and possibly site-isolation of the catalytic sites played roles in the observed differences in catalytic efficiency.²²

Although we demonstrated here and in our previous article²² that the concentration of grafted organic groups on mesoporous materials depends on the solvent used, the exact distribution and the degree of site-isolation of the functional groups has so far not been known. Here we also report a new, simple colorimetric method for elucidating the degree of site-isolation of organic groups grafted on mesoporous materials, which was demonstrated on these organoamine-grafted mesoporous materials synthesized in various solvents. We further prove that optimum grafting of catalytic sites and enhanced catalytic efficiency can be achieved by proper choice of grafting solvents. The method relies on the different complexes Cu^{2+} ions form with organoamines grafted on MCM-41 with various solvents and the characteristic colors and absorption maxima (λ_{max}) the resulting materials give. The colors and the λ_{max} were then used to characterize the degree of site-isolation of the organoamines.

For this study, excess amount of APTS was grafted on MCM-41 in methanol, isopropanol, and toluene to result in samples AP-M, AP-I, and AP-T, respectively (Scheme 1). Similarly, AAPTSS was grafted to result in AAP-M, AAP-I, and AAP-T, respectively. Our results above indicated that amino-organosilane grafting in methanol, isopropanol, and toluene resulted in ~1, 2, and 3 mmol of AP groups, respectively. While the same solvent resulted in similar numbers of AAP groups, the AAPTSS-grafted samples had twice as many amines as the corresponding APTS-grafted samples. Additional samples were synthesized by grafting 1 and 2 mmol of APTS and AAPTSS in toluene, giving AP-MT, AP-IT, AAP-MT, and AAP-IT. The latter samples have extents of organoamine grafting similar to those of AP-M, AP-I, AAP-M, and AAP-I, respectively, but with a possible difference in the degree of site-isolation or distribution of the organoamines.

We measured the d–d electronic spectrum of Cu^{2+} complexes formed in the reaction of $[\text{Cu}(\text{H}_2\text{O})_6]^{2+}$ with the various amine-functionalized mesoporous silica. Since the absorption spectra of Cu^{2+} –amine-type complexes is well understood, the location of λ_{max} for the complex provides useful information on the number and arrangement of amine ligands on the copper ion.^{4a,53} In order to probe the relative proximities of primary amine groups attached to the silica matrix produced by grafting in different solvents, $[\text{Cu}(\text{H}_2\text{O})_6]^{2+}$ was added systematically to aqueous suspensions of AP-M, AP-I, AP-T, AP-MT, and AP-

(51) Xu, T.; Zhang, J. H.; Haw, J. F. *J. Am. Chem. Soc.* **1995**, *117*, 3171–3178.

(52) Imine-supported materials are reported to act as solid base catalysts. For example, see: (a) Utting, K. A.; Macquarrie, D. J. *New J. Chem.* **2000**, *24*, 591–595. (b) Fini, F.; Sgarzani, V.; Pettersen, D.; Herrera, R. P.; Bernardi, L.; Ricci, A. *Angew. Chem., Int. Ed.* **2005**, *44*, 7975–7978. (c) Brunel, D. *Microporous Mesoporous Mater.* **1999**, *27*, 329–344.

(53) Yokoi, T.; Yoshitake, H.; Yamada, T.; Kubota, Y.; Tatsumi, T. *J. Mater. Chem.* **2006**, *16*, 1125–1135.

Table 3. λ_{\max} Values for Cu^{2+} -Metalated Organoamine-MCM-41^a

sample	μmol of $[\text{Cu}(\text{H}_2\text{O})_6]^{2+}$ for 20 mg of different organoamine-functionalized samples					E (excess, 0.05 M)
	1 (5 μmol)	2 (10 μmol)	3 (15 μmol)	4 (20 μmol)	5 (80 μmol)	
AP-M	718	717	718	717	716	718
AP-I	710	710	710	710	719	719
AP-T	628	675	655	706	713	716
AP-MT	716	717	712	710	714	
AP-IT	718	713	714	715	710	
AAP-M	651	652	652	652	681	684
AAP-I	590	614	615	615	678	683
AAP-T	594	594	598	596	661	665
AAP-MT	580	601	628	674	676	
AAP-IT	591	612	632	662	656	

^a AP- and AAP-MCM-41 were stirred in $[\text{Cu}(\text{H}_2\text{O})_6]^{2+}$. Typically, 20 mg of AP-M (12 μmol of AP) was stirred in 5, 10, 20, 40, and 80 μmol of $[\text{Cu}(\text{H}_2\text{O})_6]^{2+}$ for 1 h, giving samples AP-M-1, AP-M-2, AP-M3, AP-M4, and AP-M5, respectively. AP-M was stirred in excess (0.05 M) $[\text{Cu}(\text{H}_2\text{O})_6]^{2+}$ solution for 12 h, giving sample AP-M-E.

Table 4. λ_{\max} Values for Solutions and Precipitates Obtained by Stirring APTS and AAPTS with Cu^{2+} for 1 h (Figure S7)

organoamine	ratio of mmol of organoamine: mmol of Cu^{2+} ^a					
	8:1	4:1	2:1	1:1	1:2	1:4
APTS ^b	702	702	~680	785	803	
AAPTS		577	581	638	710	760

^a The Cu^{2+} solution and APTS (or AAPTS) were sonicated for 5 min and then kept for 1 h without sonication. ^b Most of the resulting solutions contained some precipitates because of the hydrolysis and condensation of APTS in water.

IT having the same and different extents of grafting, and the system was allowed to reach equilibrium (Table 3, Figure 6, 7, and Figures S9–S11). The studies were started with $r_t < \sim 1$, where $r_t = [[\text{Cu}(\text{H}_2\text{O})_6]^{2+}]/[\text{amine}]$, ensuring that only the highest-affinity binding sites on the functionalized mesoporous silica were bound by Cu^{2+} and favoring mononuclear complexes. Stirring the solutions for 10 min was found to be enough to get to equilibrium, but we typically stirred the solutions for 1 and 12 h (Figure S12). The metalated solids were washed with ethanol and dried, and their reflectance spectra were obtained (Table 3 and Figures 7, S9, and S10). This was done for AAP samples, too. It is worth mentioning that, while most of the Cu^{2+} -treated samples showed well-ordered mesostructures, samples stirred in excess Cu^{2+} for 12 h showed less intense Bragg peaks (Figures 6 and S8) due to the loss of mesostructures, possibly by excessive metal-chelate formation.

As is evident from the spectra shown in Figures 7, S9, and S10, AP-M-Cu and AP-I-Cu exhibit d–d absorption maxima which are shifted to higher wavelengths (λ_{\max} at 718 and 710 nm, respectively) relative to that of AP-T-Cu (λ_{\max} at 628 nm) at corresponding values of low r_t . Similarly, AAP-M-Cu exhibits a d–d absorption maximum which is shifted to higher wavelengths (λ_{\max} at 650 nm) relative to those of AAP-I-Cu and AAP-T-Cu (λ_{\max} at 590 and 594 nm, respectively) at corresponding values of r_t (Table 3). This shows that the average crystal field about the Cu^{2+} ion in AP-M-Cu and AP-I-Cu must be lower than the average crystal field of AP-T-Cu. Similarly, the average crystal field about the Cu^{2+} ion in AAP-M-Cu must be lower than the average crystal field of AAP-I-Cu and AAP-T-Cu. Since amines have higher crystal field strength than H_2O , this indicates that more amines are bound to the Cu^{2+} in AP-T than AP-M and AP-I (or in AAP-T than AAP-M and AAP-I). Interestingly, AAP-MT and AAP-IT gave lower λ_{\max} (~590 nm)

than AAP-M and AAP-I (~655 nm), respectively. In view of the fact that the percentage of grafting is approximately the same in the latter materials compared, Cu^{2+} ions binding in AAP-MT and AAP-IT clearly have access to more closely lying amine groups than they do in either AAP-M and AAP-I. This indicates that the distribution of grafted groups is solvent-dependent and that grafting in toluene produces “clusters” of grafted AAP groups, while the analogous process carried out in the alcohols yields grafted groups which are relatively isolated from one another.^{4a} Thus, the copper environment in AAP-MT and AAP-IT is more consistent with a CuN_4O_2 -type structure, while the corresponding environment in AAP-M and AAP-I is of CuN_2O_4 -type structure. A similar trend was, however, not observed when comparing AP-MT and AP-IT with AP-M and AP-I, respectively. This was probably because there is only one amine group in the AP functional groups compared to AAP, and so a hydrogen-bonded aggregate of APTS in toluene is less likely than that of AAPTS, especially with the low concentrations of APTS and AAPTS used in the grafting of these samples (see Experimental Section). Thus, the structure in AP-M, AP-I, AP-MT, and AP-IT was mostly of CuNO_5 type. As r_t increases, the Cu d–d transition is red-shifted in most samples, indicating the formation of a polynuclear complex, CuNO_5 , at the expense of mononuclear ones, CuN_2O_4 and CuN_4O_2 . These structure assignments are supported by λ_{\max} values of similar complexes synthesized in solution from known ratios of $[\text{Cu}(\text{H}_2\text{O})_6]^{2+}$ and ammonia, ethylenediamine,^{54,55} APTS, or AAPTS (Figure 8 and Table 4). The slight differences observed between the λ_{\max} of the solid and the solutions can be explained by the fact that basic silanol groups are able to replace H_2O in $[\text{Cu}(\text{H}_2\text{O})_6]^{2+}$. This is the first time copper–amine complexes on amine-grafted mesoporous materials synthesized in various solvents were studied and their degree of site-isolation with the electronic spectrum was established. Previous recent studies by Voss et al.⁵⁶ and Jana et al.⁵⁷ have focused on different materials, and also they did not carry out such studies. On the basis of our results, we obtain the model structures shown in Scheme 3 for metalated samples, with different degrees of site-isolated amine groups.

The colors of the samples also revealed an interesting trend. While AP-M-Cu and AP-I-Cu gave a light blue color, AP-T-Cu gave a purple color (Figures 9 and S12). Similarly, while AAP-M and AAP-I gave a light purple color, AAP-T gave a very deep purple color. These colors correspond to the different types of Cu–amine complexes. For instance, CuN_4O_2 complexes give a characteristic deep purple color, while CuN_2O_4 complexes give a faint blue color.⁵⁸ Therefore, this colorimetric method, involving addition of a small amount of dilute Cu^{2+} solution to functionalized mesoporous materials, and the different colors

- (54) (a) Gaspar, M.; Telo, J. P.; Santos, M. A. *Eur. J. Inorg. Chem.* **2003**, 4025–4034. (b) Chacko, S.; Mathew, T.; Kuriakose, S. *J. Appl. Polym. Sci.* **2003**, *90*, 2684–2690. (c) Yesilel, O. Z.; Olmez, H.; Soyulu, S. *Transition Metal Chem.* **2006**, *31*, 396–404. (d) Mimmi, M. C.; Gullotti, M.; Santagostini, L.; Battaini, G.; Monzani, E.; Pagliarini, R.; Zoppellaro, G.; Casella, L. *Dalton Trans.* **2004**, 2192–2201.
- (55) Itoh, S.; Taniguchi, M.; Takada, N.; Nagatomo, S.; Kitagawa, T.; Fukuzumi, S. *J. Am. Chem. Soc.* **2000**, *122*, 12087–12097.
- (56) Voss, R.; Thomas, A.; Antonietti, M.; Ozin, G. A. *J. Mater. Chem.* **2005**, *15*, 4010–4014.
- (57) Jana, S.; Dutta, B.; Bera, R.; Koner, S. *Langmuir* **2007**, *23*, 2492–2496.
- (58) (a) Fischmann, A. J.; Warden, A. C.; Black, J.; Spiccia, L. *Inorg. Chem.* **2004**, *43*, 6568–6578. (b) Kaur, N.; Kumar, S. *Dalton Trans.* **2006**, 3766–3771. (c) Lee, Y. M.; Lee, H. W.; Kim, Y. I. *Polyhedron* **2005**, *24*, 377–382. (d) Balamurugan, R.; Palaniandavar, M.; Gopalan, R. S. *Inorg. Chem.* **2001**, *40*, 2246–2255.

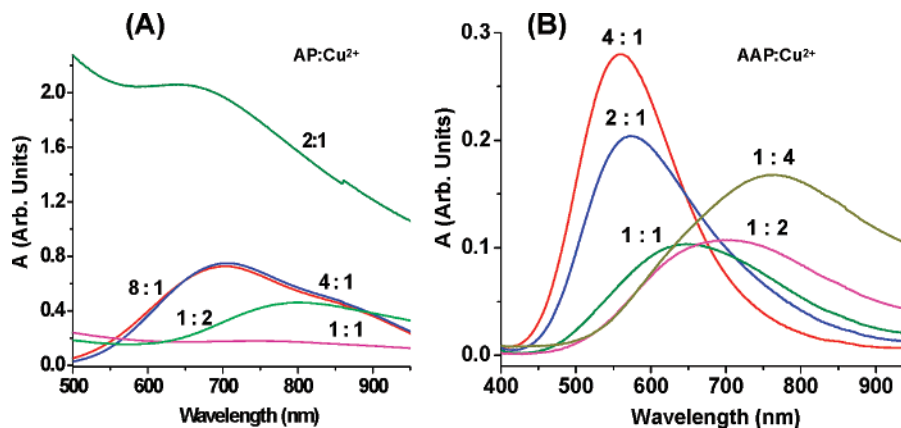


Figure 8. UV-vis absorption and reflectance spectra of control samples. (A) Cu^{2+} and APTS were mixed in various APTS: Cu^{2+} mole ratios, and the precipitates (in the case of precipitate formation) or the solutions (in the case of no precipitate formation) were measured. (B) Cu^{2+} and AAPTS were mixed in various AAPTS: Cu^{2+} mole ratios, and the solutions formed were measured.

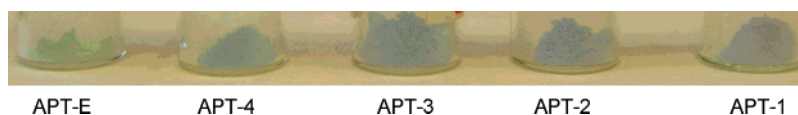
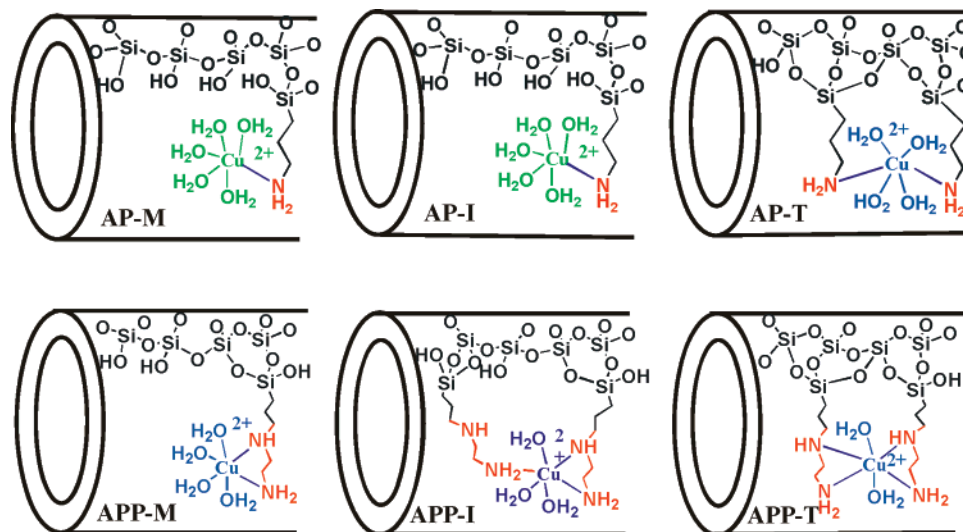


Figure 9. Digital images of a series of representative Cu^{2+} -metalated amine-functionalized mesoporous materials obtained by mixing Cu^{2+} with APT-functionalized mesoporous samples.

Scheme 3. Complexation of Cu^{2+} with Different Degrees of Site-Isolated Organoamines Grafted in Various Solvents (M = Methanol, I = Isopropanol, and T = Toluene) Will Give Different Colors or λ_{max}



and λ_{max} of the resulting samples can be used as a rapid and simple way to determine the degree of site-isolation of functional groups on solid nanoporous materials.

4. Conclusions

In conclusion, we have performed a comprehensive study and found a strong correlation between polarity and dielectric constant of solvents used for grafting organic groups onto mesoporous materials and the structures and catalytic properties of the organic-functionalized materials. The grafting density and site-isolation of the functional groups and their catalytic properties can be optimized by judicious choice of solvents. This will allow synthesis of efficient, functionalized mesoporous catalysts. The degree of site-isolation or distribution of the organic functional groups was elucidated by a simple colorimetric technique we demonstrated, which employed measure-

ment of electronic spectra of the d-d transition of the Cu^{2+} complexes produced by stirring the organoamine-grafted mesoporous materials in dilute aqueous Cu^{2+} solution.

Acknowledgment. We thank the U.S. National Science Foundation, CAREER Grant No. CHE-0645348, for financially supporting this work. We also thank Prof. James C. Dabrowiak for very valuable discussion.

Supporting Information Available: N_2 BET gas adsorption and BJH pore-size distributions, tables of solid-state NMR data, solid-state NMR spectra, UV-vis electronic spectra, and digital images of Cu^{2+} -complexed amino-functionalized mesoporous materials (Table S1, Figures S1-S13). This material is available free of charge via the Internet at <http://pubs.acs.org>.

JA074128T